Proceedings of the 9ICEG
9th International Congress on Environmental Geotechnics
25-28 June, 2023 | Chania, Greece

https://doi.org/10.53243/ICEG2023-146

Liquefaction response of pond ash with varying bottom ash content

Sujay Teli[1], and Ajanta Sachan[2]

[1]*Research Scholar, Indian Institute of Technology, Gandhinagar, India, email: teli_sujay@iitgn.ac.in*

[2]*Associate Professor, Indian Institute of Technology, Gandhinagar, India, email: ajanta@iitgn.ac.in*

ABSTRACT

The deposition process of ash slurry in the disposal site results in segregation of bottom ash and fly ash particles. Pond ash collected from different locations of the same disposal site can have varying proportions of bottom ash and fly ash particles. The present study evaluates the effect of varying bottom ash content on the liquefaction response of pond ash. A series of stress-controlled cyclic simple shear (CSS) tests were performed on pond ash with varying bottom ash content (0%, 20%, 40%, and 50%). The loading cycles were applied in the sinusoidal form at 1 Hz frequency and 0.12 cyclic stress ratio (CSR) under 100 kPa vertical overburden stress. All the specimens were prepared at their respective 95% maximum dry density (MDD) and optimum moisture content (OMC). The number of loading cycles required to liquefy the specimen was evaluated based on two criteria: i) Excess pore water pressure ratio, $r_u \geq 0.9$, and ii) Double amplitude shear strain, $\gamma_{DA} \geq 7.5\%$. Dynamic properties such as shear modulus (G) and damping ratio (D) were also evaluated for pond ash with varying bottom ash content. It was observed that the liquefaction resistance increased with an increase in bottom ash content. The generation of shear strain with the number of loading cycles was found to be more gradual with an increase in bottom ash content. The specimen with 0% bottom ash content showed a sharp decrease in shear modulus with an increasing number of loading cycles as compared to the specimen with 50% bottom ash content.

Keywords: Pond ash, bottom ash, liquefaction, excess pore water pressure ratio, double amplitude shear strain, shear modulus

1 INTRODUCTION

Thermal power plants in India produce a large amount of coal ash as a by-product of electricity generation. Two types of ashes are generated from burning coal: bottom ash and fly ash. Bottom ash acquires 20% of the total coal ash, whereas fly ash acquires 80% of the total coal ash. Over 60% of fly ash is used in cement manufacturing, concrete and other industries. The unutilized fly ash is mixed with bottom ash with water to form a slurry and transported to the ash disposal site of the thermal power plant hydraulically through large pipes. With time the ash mixture gets deposited at a disposal site. The ash sample collected from the disposal site is known as pond ash. When the ash mixture is transported to the disposal site, segregation of particles occurs. Coarse bottom ash particles (particle size>75 micron) settle near the inflow point of disposal site and finer fly ash particles (particle size<75 micron) settle away from the inflow point. This segregation results in the variation of particle size gradation throughout the disposal site, which leads to different geotechnical properties of pond ash collected from different locations of the same disposal site (Jakka et al., 2010b).

Pond ash is used in many geotechnical structures as fill material, such as highway embankments, railway embankments, bridge approach embankments etc. (Kim et al., 2005; Jakka et al., 2010b; Awang et al.,2011). Many researchers observed that pond ash is highly susceptible to liquefaction (Zand et al., 2009; Jakka et al., 2010a; Mohanty and Patra, 2014; Mohanty and Patra, 2016). During an earthquake, there can be severe damage to embankments or any geotechnical structure made with pond ash as fill material. The liquefaction response of pond ash should be evaluated for structures constructed in earthquake-prone areas. Only a few previous studies accommodated the effect of particle size variation in the same disposal site by collecting samples from inflow and outflow points (Jakka et al., 2010a; Singh and Singh, 2022). Hence, a detailed investigation on the effect of bottom ash content on liquefaction response and dynamic properties of pond ash from a given disposal site is needed. The current study evaluated the liquefaction response of pond ash with varying bottom ash content. In previous studies,

cyclic triaxial tests were used to evaluate the effect of variation in particle gradation on the liquefaction response of pond ash. However, effect of bottom ash content on liquefaction response of pond ash using cyclic simple shear (CSS) test is yet to be explored. CSS provides better simulation of field conditions during an earthquake by providing a horizontal direction of shearing under vertical overburden stress. Hence, in this study, a series of stress-controlled CSS tests were performed to evaluate the effect of varying bottom ash content on the liquefaction response of pond ash. Bottom ash (BA) content was varied as 0%, 20%, 40% and 50%. Liquefaction response was studied based on the number of loading cycles required to initiate liquefaction. Dynamic properties such as shear modulus (G), damping ratio (D) and cyclic degradation index (δ) were also evaluated.

2 MATERIAL PROPERTIES AND EXPERIMENTAL PROGRAM

2.1 Material properties and specimen preparation

In the current study, pond ash was collected from the disposal site of the Gandhinagar thermal power plant. Varioius combinations of fly ash(<75 micron) and bottom ash (size> 75 micron) were used to study the effect of bottom ash content on liquefaction respons of pond ash.

Table 1. *Geotechnical properties of pond ash with varying bottom ash content*

%Bottom ash (>75 μ)	%Fly ash (<75 μ)	Specific gravity	MDD (g/cm^3)	OMC (%)	Φ (degrees)
0%	100%	2.23	1.39	21	31
20%	80%	2.23	1.37	22	31
40%	60%	2.24	1.34	22	31
50%	50%	2.24	1.32	23	33

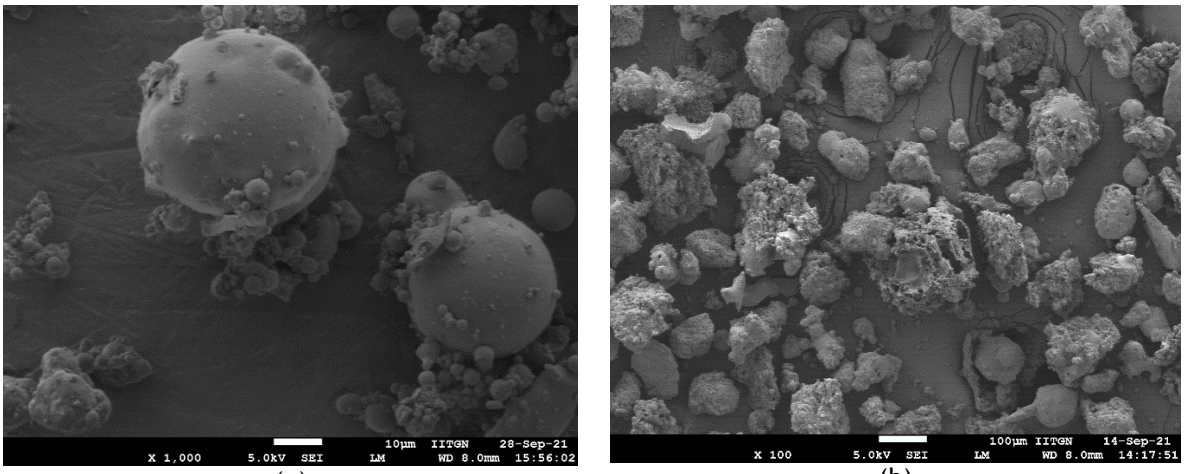

(a) (b)

Figure 1. *SEM images of (a)Fly ash and (b) Bottom ash*

The basic geotechnical properties of pond ash with varying bottom ash (BA) content are presented in Table 1. MDD and OMC were obtained using the standard proctor test. Direct shear tests were performed on the saturated pond ash specimens to obtain shear strength parameters cohesion (c) and angle of internal friction (φ). All pond ash specimens were found to be cohesionless. Scanning electron microscopy was performed to evaluate the particle shape and structure. SEM images of bottom ash and fly ash particles are shown in Figure 1. It can be observed from the figure that bottom ash particles were irregular in shape and had a rough surface texture. Also, some bottom ash particles showed intra-particle voids and angular shapes. In contrast, fly ash particles had spherical particles with smooth surface texture.

The CSS tests were performed on the specimens of 20 mm height and 70 mm diameter for each pond ash sample. All the specimens were prepared at their 95% of MDD and OMC obtained by standard proctor test. The moist tamping method was used to prepare the specimens in three layers of similar height in a cylindrical mold. After preparing the specimen, it was transferred to cyclic simple shear apparatus with minimal disturbance from the mold.

2.2 Cyclic simple shear (CSS) test

A series of stress-controlled CSS tests was performed on the specimens of pond ash with varying bottom ash content. Electro-mechanically controlled CSS test equipment had capacity of producing the cyclic loading upto 5Hz frequency. It was equipped with a vertical load cell of 5 kN capacity with a vertical LVDT. It had a horizontal load cell mounted directly on the specimen assembly to avoid any additional frictional resistance during cyclic loading with a horizontal LVDT. Firstly, the specimens were saturated by passing water through the specimen for 24 hours at vertical seating pressure of 10 kPa. Saturation was assured by measuring the water conent of the specimen after shearing. After saturation, the specimens were consolidated at 100 kPa vertical overburden stress until the vertical deformation became constant. Subsequently, cyclic loading was applied to shear the specimens in horizontal direction. The input loading cycles (Figure 2) were applied in the sinusoidal form at 1 Hz frequency and 0.12 cyclic stress ratio (CSR) to simulate earthquake loading conditions.

.

CSR for stress-controlled CSS test is defined as,

$$CSR = \tau_{peak} / \sigma_{vertical} \quad (1)$$

Where τ_{peak} is the amplitude of input shear stress loading and $\sigma_{vertical}$ is the applied vertical overburden pressure.

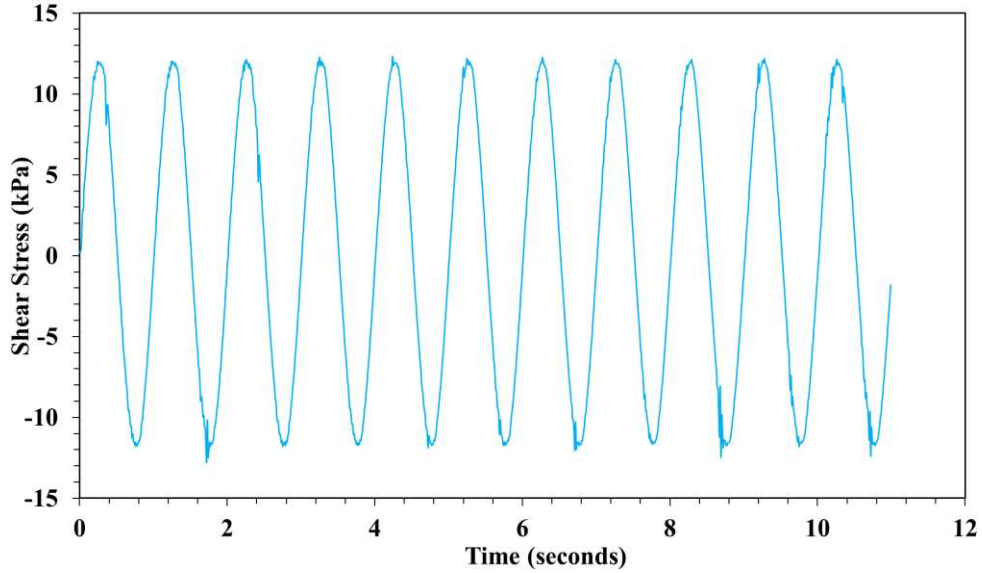

Figure 2. *Input loading for stress-controlled CSS test (Amplitude- 12 kPa and Frequency- 1Hz)*

Loading was continued until the specimen attained a double amplitude shear strain (γ_{DA}) value of 7.5%. The excess pore water pressure generated during shearing was measured indirectly by evaluating the reduction in the vertical overburden stress.

3 RESULTS AND DISCUSSION

3.1 Results

Figure 3 represents the hysteresis loops for the first fifteen loading cycles for pond ash with 0% to 50% BA content. The figure shows that after 15 loading cycles, hysteresis loop became wider for the pond ash specimen with 0% BA content compared to the specimen with 50% BA content. Hence, indicating the generation of higher shear strain in specimen with 0% BA content than in specimen with 50% BA content.

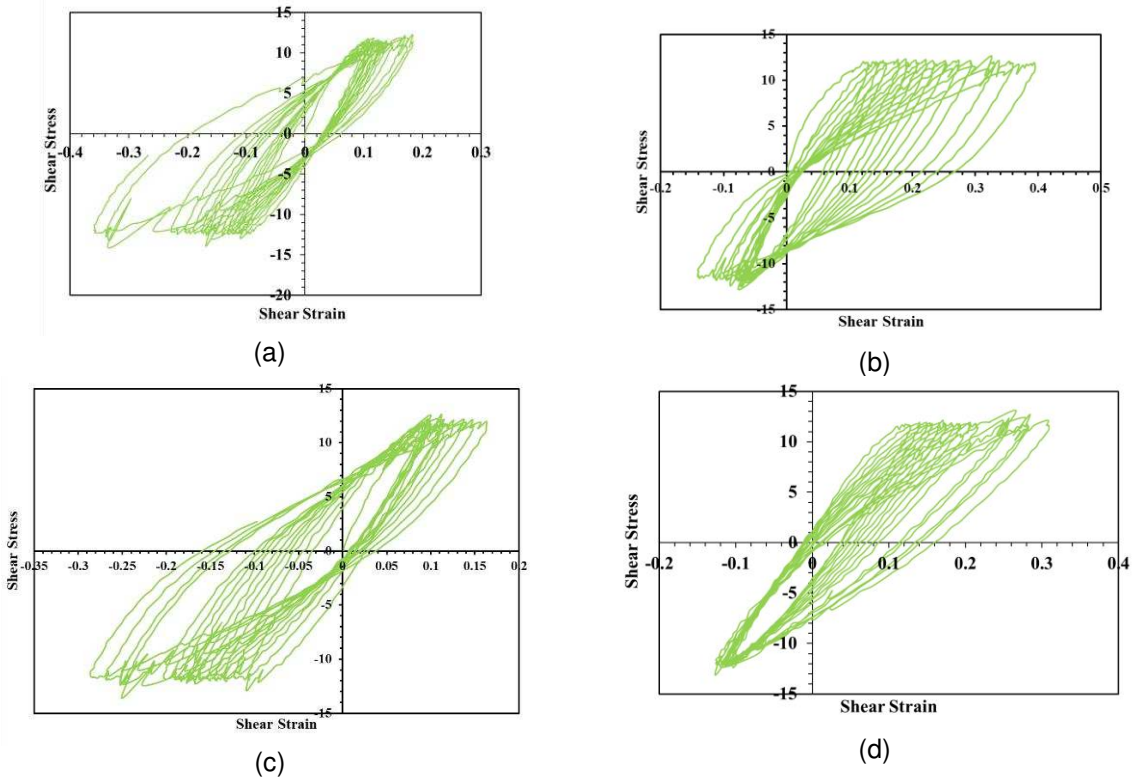

Figure 3. *Hysteresis loop of pond ash for first 15 loading cycles, (a) 0% BA content, (b) 20% BA content, (c)40% BA content and (d) 50% BA content*

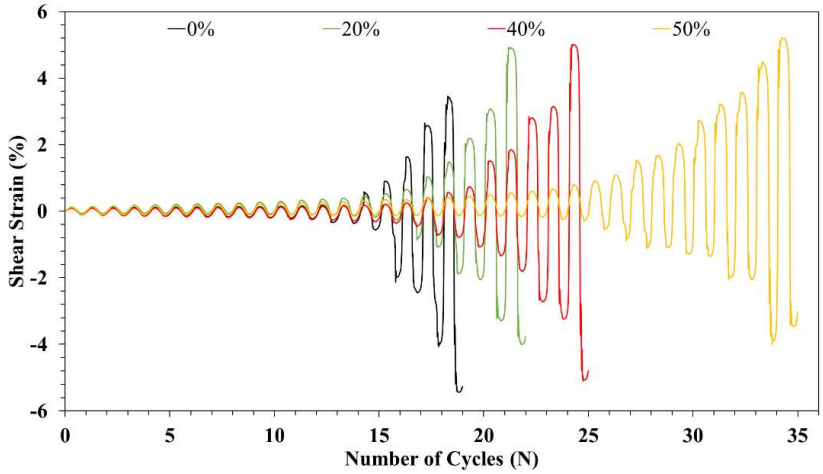

Figure 4. *Development of shear strain in pond ash under cyclic loading with varying bottom ash content*

Figure 4 represents the shear strain response of pond ash with varying bottom ash content. The figure shows that each specimen generated negligible shear strain at initial loading cycles (N≤10). Sudden development of large shear strains was observed for the specimens with BA content of 0%, 20% and 40% after 10-15 loading cycles. The specimen with 50% BA content showed a gradual increase in the shear strain values with the number of loading cycles. The number of loading cycles required to generate large shear strains increased with an increase in bottom ash content.

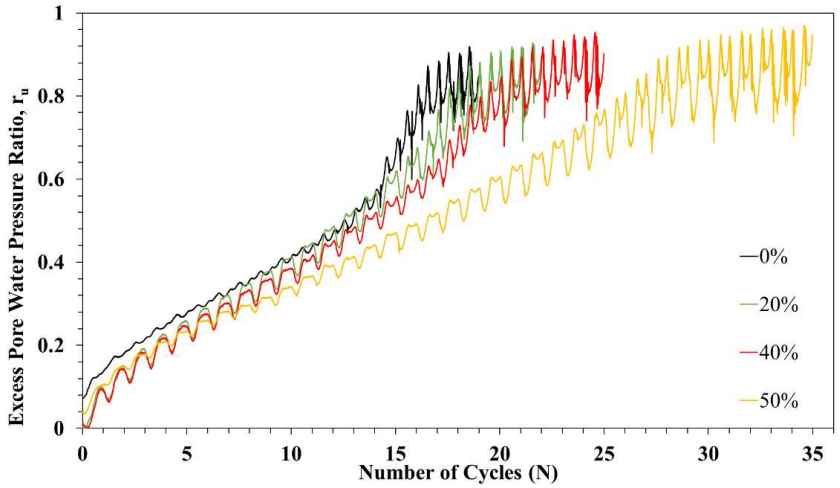

Figure 5. *Development of excess pore water pressure in pond ash under cyclic loading with varying bottom ash content*

The excess pore water pressure response of pond ash specimens with varying bottom ash content is shown in Figure 5. The results are presented in the form of excess pore water pressure ratio (r_u), defined as the ratio of excess pore water pressure to the initial vertical overburden pressure. Figure 5 exhibited that the number of loading cycles required to generate $r_u \geq 0.9$ increased with an increase in bottom ash content. For all specimens, it was observed that for a particular loading cycle, r_u approached its maximum value momentarily and then reduced to some residual value at the end of the cycle. This behavior can be attributed to the fact that the specimens were in dense condition. Sudden development of excess pore water pressure was observed for specimens with bottom ash content ≤ 40% after ten loading cycles. For specimens with 50% BA content, pore pressure development was observed to be gradual with the number of loading cycles.

Two criteria were used to define liquefaction in the present study as follows: i) Excess pore water pressure ratio, $r_u \geq 0.9$, and ii) Double amplitude shear strain, $\gamma_{DA} \geq 7.5\%$. Double amplitude strain for a particular loading cycle can be defined as the total peak-to-peak shear strain. Figure 6 depicts the generation of double amplitude shear strain (γ_{DA}) with the number of loading cycles for pond ash with varying bottom ash content. The figure depicted that the number of loading cycles required to reach higher double amplitude shear strains increased with the bottom ash content. It can be observed from the figure that double amplitude shear strains were found to be negligible at initial loading cycles until a sudden development of large double amplitude shear strains was observed for BA content ≤ 40%.

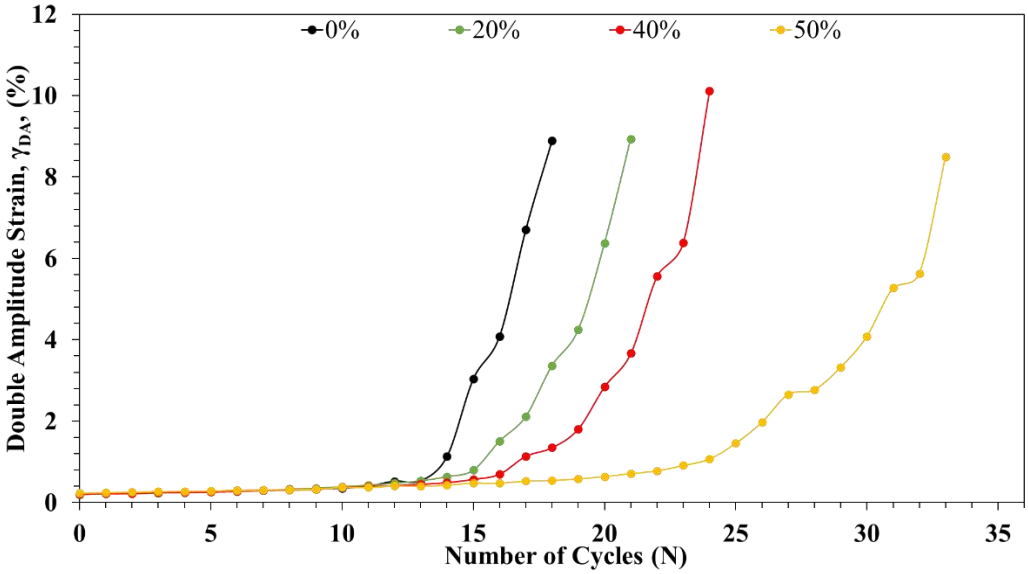

Figure 6. *Development of double amplitude shear strain in pond ash under cyclic loading with varying bottom ash content*

Figure 7 represents the behavior of the cyclic degradation index with the number of loading cycles for pond ash with varying bottom ash content. The cyclic degradation index (δ) for a particular loading cycle is the ratio of the shear modulus of the particular cycle (G) to the shear modulus of the specimen in first cycle (G_0). It can be given as,

$$\delta = G/G_0 \quad (2)$$

From the figure, it can be observed that degradation of pond ash was found to be rapid for specimens with bottom ash content ≤ 40% as compared to specimens with 50% bottom ash content

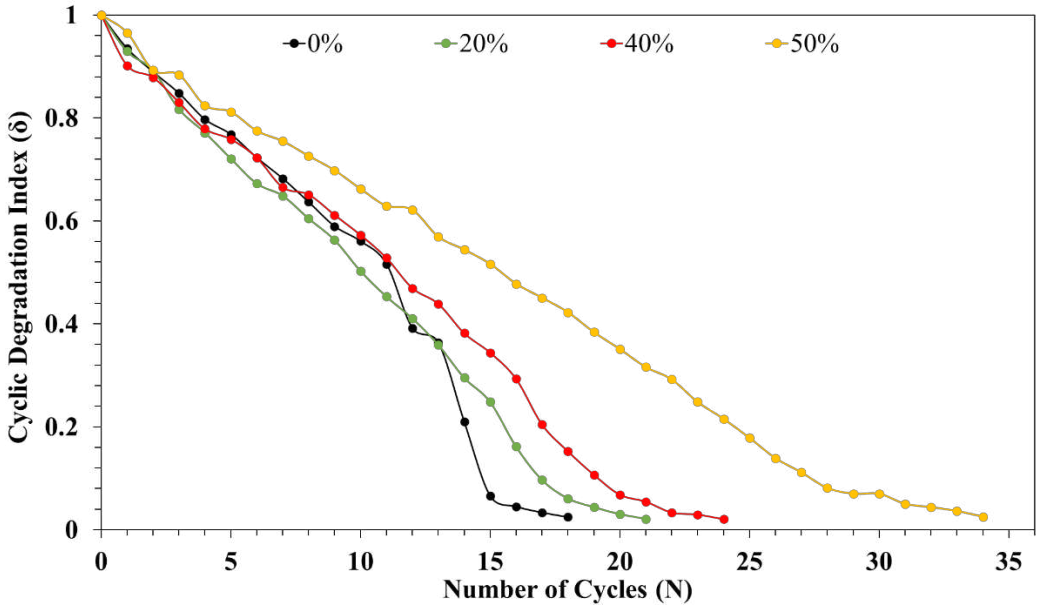

Figure 7. *Cyclic degradation index of pond ash under with varying bottom ash content*

Table 2 represents the dynamic properties of pond ash with varying bottom ash content for the 1st loading cycle and 15th loading cycle, along with the number of loading cycles required to initiate the liquefaction (N_L) in the specimen. It can be observed from the table that, for the first cycle, shear modulus G remained almost constant with an increase in bottom ash content up to 40%. G decreased with a further increase in bottom ash content at 50%. The decrease in G after the first fifteen loading cycles was considerable for pond ash with 0% bottom ash content. Whereas, with an increase in bottom ash content, degradation of G was reduced. Damping ratio was observed to be nearly constant, with an increase in bottom ash content for the first cycle. After 15 loading cycles also, it remained nearly constant. Double amplitude shear strain was minimal for each specimen and found to be constant with an increase in bottom ash content for the first loading cycle. After 15 loading cycles, double amplitude shear strain showed a considerable increase for specimen with 0% bottom ash content.

The number of loading cycles required to initiate liquefaction increased with an increase in bottom ash content for both criteria. Therefore, specimen with 0% bottom ash content was more susceptible to liquefaction. For specimens with bottom ash content ≤ 20% value of N_L was similar for both criteria. With an increase in the bottom ash content value of N_L from criterion, $\gamma_{DA} \geq 7.5\%$ was observed to be higher than criterion $r_u \geq 0.9$.

Table 2. *Dynamic properties of pond ash with varying bottom ash content for 1st and 15th loading cycle*

%BA	For 1st Cycle			For 15th Cycle			N_L ($r_u \geq 0.9$)	N_L ($\gamma_{DA} \geq 7.5\%$)
	G (kPa)	D (%)	γ_{DA} (%)	G (kPa)	D (%)	γ_{DA} (%)		
0	11769	15.1	0.20	774	18.2	3.04	18	19
20	11893	16.6	0.19	2956	18.0	0.80	20	21
40	11929	15.1	0.21	4104	17.6	0.57	22	25
50	10123	15.0	0.23	5227	16.2	0.48	28	34

3.2 Discussion

It was observed that the development of shear strain, degradation of shear modulus and liquefaction susceptibility was reduced with an increase in bottom ash content. Pond ash can be considered as a mixture of sand and silt-sized particles. For sand-silt mixture, many researchers (Thevanayagam et al., 2002; Dash and Sitharam, 2011; Porcino and Diano, 2017) observed that the strength of soil matrix is governed by silt-silt interaction after a certain amount of silt content, known as threshold silt content. Before threshold silt content, the soil matrix is governed by sand-sand particle interaction. The concept of intergranular void ratio was used to define the threshold silt content. The intergranular void ratio can be defined as,

$$e_g = \frac{e + fc}{1 - fc} \tag{3}$$

Where e_g is the intergranular void ratio, e is the void ratio of the soil matrix, f_c is the ratio of fines or silt content to 100.

When the intergranular void ratio e_g of the sand-silt mixture, becomes greater than the maximum void ratio of sand ($e_{max(sand)}$), the strength of the soil matrix is governed by silt particles, which results in a decrease of liquefaction resistance. Pond ash specimens can be considered similar to sand-silt mixtures, where fly ash represents silt and bottom ash represents sand. The maximum void ratio of bottom ash ($e_{max(BA)}$) was measured by funnel deposition from a constant height and was found to be 1.7. Intergranular void ratio after consolidation for 20%, 40% and 50% bottom ash content was found to be 7.256, 3.156 and 2.384, respectively. Hence, for each specimen $e_g > e_{max(BA)}$, indicating that the interaction of fly ash-fly ash particles governs the liquefaction response of pond ash. With the increase in bottom ash content, bottom ash acts as a reinforcing agent in fly ash-dominated pond ash matrix. As shown in Figure 1, bottom ash particles were irregular in shape, having angular particles and rough surface texture that provided good frictional resistance. Hence, with an increase in bottom ash content liquefaction susceptibility and cyclic degradation of pond ash were reduced.

4 CONCLUSIONS

In this study, a series of stress-controlled CSS tests were performed to evaluate the effect of bottom ash content on the liquefaction response of pond ash. It was observed that considerable shear strain ($\gamma_{DA} \geq 7.5\%$) was generated in all pond ash specimens before the excess pore water pressure ratio, r_u became 1. All the specimens showed minimal shear strain at initial loading cycles. Specimens with BA content ≤ 40% showed a sudden increase in shear strain after 10 loading cycles. With an increase in bottom ash content, excess pore water pressure development became more gradual with the number of loading cycles. A high double amplitude shear strain value accompanied the high excess pore water pressure in each specimen. With the increase in bottom ash content, higher double amplitude shear strain was observed at a higher number of loading cycles, indicating increased resistance to deformation. The cyclic degradation of specimen with the number of loading cycles became steeper with a decrease in bottom ash content. The damping ratio of specimens remained almost constant with

an increase in bottom ash content. The number of loading cycles required to initiate the liquefaction increased with an increase in bottom ash content. Hence, the pond ash specimen with 0% BA content was more susceptible to liquefaction.

REFERENCES

Awang, A. R., Marto, A., & Makhtar, A. M. (2011). Geotechnical properties of Tanjung Bin coal ash mixtures for backfill materials in embankment construction. *Ejge, 16, s*1515-1531.

Chattaraj, R., & Sengupta, A. (2017). Dynamic properties of fly ash. *Journal of Materials in Civil Engineering*, *29*(1), 04016190.

Dash, H. K., & Sitharam, T. G. (2011). Undrained cyclic and monotonic strength of sand-silt mixtures. *Geotechnical and Geological Engineering*, *29*(4), 555-570.

Jakka, R. S., Datta, M., & Ramana, G. V. (2010a). Liquefaction behavior of loose and compacted pond ash. *Soil Dynamics and Earthquake Engineering*, *30*(7), 580-590.

Jakka, R. S., Ramana, G. V., & Datta, M. (2010b). Shear behaviour of loose and compacted pond ash. *Geotechnical and Geological Engineering*, *28*(6), 763-778.

Karim, M. E., & Alam, M. J. (2014). Effect of non-plastic silt content on the liquefaction behavior of sand–silt mixture. *Soil Dynamics and Earthquake Engineering*, *65*, 142-150.

Kim, B., Prezzi, M., & Salgado, R. (2005). Geotechnical properties of fly and bottom ash mixtures for use in highway embankments. *Journal of Geotechnical and Geoenvironmental Engineering*, *131*(7), 914-924.

Mohanty, S., & Patra, N. R. (2014). Cyclic behavior and liquefaction potential of Indian pond ash located in seismic zones III and IV. *Journal of materials in civil engineering*, *26*(7), 06014012.

Mohanty, S., & Patra, N. R. (2016). Dynamic response analysis of Talcher pond ash embankment in India. *Soil Dynamics and Earthquake Engineering*, *84*, 238-250.

Polito, C. P., & Martin II, J. R. (2001). Effects of non-plastic fines on the liquefaction resistance of sands. *Journal of geotechnical and geoenvironmental engineering*, *127*(5), 408-415.

Porcino, D. D., & Diano, V. (2017). The influence of non-plastic fines on pore water pressure generation and undrained shear strength of sand-silt mixtures. *Soil Dynamics and Earthquake Engineering*, *101*, 311-321.

Singh, J., & Singh, S. K. (2022). Dynamic Properties of Spatially-Varied Pond Ash within a Coal Ash Pond. *International Journal of Geomechanics*, *22*(3), 04021309.

Thevanayagam, S., & Mohan, S. (2000). Intergranular state variables and stress–strain behaviour of silty sands. *Geotechnique*, *50*(1), 1-23.

Thevanayagam, S., Shenthan, T., Mohan, S., & Liang, J. (2002). Undrained fragility of clean sands, silty sands, and sandy silts. *Journal of geotechnical and geoenvironmental engineering*, *128*(10), 849-859.

Yoshimoto, N., Orense, R. P., Hyodo, M., & Nakata, Y. (2014). Dynamic behavior of granulated coal ash during earthquakes. *Journal of Geotechnical and Geoenvironmental Engineering*, *140*(2), 04013002.

Zand, B., Tu, W., Amaya, P. J., Wolfe, W. E., & Butalia, T. S. (2009). An experimental investigation on liquefaction potential and post-liquefaction shear strength of impounded fly ash. *Fuel*, *88*(7), 1160-1166.